Physica Medica 31 (2015) 510–516

Contents lists available at ScienceDirect

Physica Medica

journal homepage: http://www.physicamedica.com

Technical notes

Monte Carlo-based assessment of the trade-off between spatial resolution, field-of-view and scattered radiation in the variable resolution X-ray CT scanner

Hossein Arabi [a], Ali Reza Kamali Asl [b], Mohammad Reza Ay [c, d], Habib Zaidi [a, e, f, *]

[a] Division of Nuclear Medicine and Molecular Imaging, Geneva University Hospital, CH-1211, Geneva, Switzerland
[b] Department of Radiation Medicine, Shahid Beheshti University, 1983963113, Tehran, Iran
[c] Research Centre for Molecular and Cellular Imaging, Tehran University of Medical Sciences, Tehran, Iran
[d] Department of Medical Physics and Biomedical Engineering, Tehran University of Medical Sciences, Tehran, Iran
[e] Geneva Neuroscience Center, Geneva University, CH-1205, Geneva, Switzerland
[f] Department of Nuclear Medicine and Molecular Imaging, University of Groningen, University Medical Center Groningen, 9700, RB Groningen, Netherlands

ARTICLE INFO

Article history:
Received 20 September 2014
Received in revised form
18 March 2015
Accepted 19 March 2015
Available online 11 April 2015

Keywords:
Variable resolution X-ray CT
Spatial resolution
Scattered radiation
Monte Carlo

ABSTRACT

Objective: The purpose of this work is to evaluate the impact of optimization of magnification on performance parameters of the variable resolution X-ray (VRX) CT scanner.
MethodsA realistic model based on an actual VRX CT scanner was implemented in the GATE Monte Carlo simulation platform. To evaluate the influence of system magnification, spatial resolution, field-of-view (FOV) and scatter-to-primary ratio of the scanner were estimated for both fixed and optimum object magnification at each detector rotation angle. Comparison and inference between these performance parameters were performed angle by angle to determine appropriate object position at each opening half angle.
Results: Optimization of magnification resulted in a trade-off between spatial resolution and FOV of the scanner at opening half angles of 90°−12°, where the spatial resolution increased up to 50% and the scatter-to-primary ratio decreased from 4.8% to 3.8% at a detector angle of about 90° for the same FOV and X-ray energy spectrum. The disadvantage of magnification optimization at these angles is the significant reduction of the FOV (up to 50%). Moreover, magnification optimization was definitely beneficial for opening half angles below 12° improving the spatial resolution from 7.5 cy/mm to 20 cy/mm. Meanwhile, the FOV increased by more than 50% at these angles.
Conclusion: It can be concluded that optimization of magnification is essential for opening half angles below 12°. For opening half angles between 90° and 12°, the VRX CT scanner magnification should be set according to the desired spatial resolution and FOV.

1. Introduction

X-ray computed tomography (CT) is a well-established structural diagnostic imaging modality widely used in clinical practice. CT scanners can provide three-dimensional images representing *in vivo* anatomy. These precious features have made it a trusted method for diagnostic purposes. Depending on the size of the object being imaged, CT scanners exhibit different field-of-view (FOV) and spatial resolution characteristics. Clinical CT scanners have a relatively large FOV of up to 50 cm for whole body imaging and moderate spatial resolution in the range of 1–3 cy/mm [1]. A decrease in object size has no effect on spatial resolution of clinical CT scanners. On the other hand, micro-CT scanners are appropriate for imaging small objects and animals. Such scanners can achieve a spatial resolution of up to 100 cy/mm. However, they suffer from the limited FOV [1].

A novel design concept referred to as the variable resolution X-ray (VRX) CT scanner was recently proposed to enable the integration of the advantages of both clinical and micro-CT scanners. In the VRX CT scanner, the spatial resolution changes according to the

* Corresponding author. Geneva University Hospital, Division of Nuclear Medicine and Molecular Imaging, CH-1211, Geneva, Switzerland. Tel.: +41 22 372 7258; fax: +41 22 372 7169.
E-mail address: habib.zaidi@hcuge.ch (H. Zaidi).

http://dx.doi.org/10.1016/j.ejmp.2015.03.014
1120-1797/

object size [2]. In such scanners, by angulation of the detector with respect to the incident X-ray beam, the apparent cells width in the object plane would decrease which consequently results in improved spatial resolution. Briefly, the spatial resolution and the FOV of the VRX CT scanner is a function of detector arm angulation [3]. The outstanding merit of the VRX CT scanner is that objects are imaged at an adequate spatial resolution according to their size. As such, small objects are imaged at high spatial resolution while the FOV is accordingly small, whereas large objects are imaged at relatively low spatial resolution and large FOV.

The idea behind the VRX CT can be applied in a variety of configurations for different purposes. In a single array VRX detector, the spatial resolution improvement is due to a decrease of the apparent size of the cells in the transverse plane while the axial spatial resolution remains unchanged. Cone-beam VRX CT can improve the spatial resolution not only in the transaxial plane but also in the axial plane. Mutli-arm VRX CT scanners are designed to scan objects at two different spatial resolutions in a single acquisition such that the target region in the object is imaged at high spatial resolution whereas the remaining area is imaged at relatively low spatial resolution. Each of these types of VRX CT scanners has its own limitations, calibration parameters and image reconstruction challenges that require detailed assessment and optimization [4].

A common physical limitation that tends to degrade the spatial resolution of VRX CT scanners is the X-ray source focal spot size [3]. In all configurations of VRX CT scanners (one-dimensional, flat panel and cone-beam), the angulation of the detector results in improvement in detector resolution while the geometrical unsharpness due to the influence of focal spot size remains unchanged [5]. In addition, the optimum magnification at each detector angle, which leads to maximum achieveable resolution, varies due to improvement in detector resolution. Two factors that contribute to optimum magnification are detector resolution and focal spot size. In the VRX CT, the detector resolution varies as a function of angle between the detector and incident X-ray beam while the focal spot size is fixed independent of detector angulation. Thus, the optimum magnification is different at each incident angle and as such, utilizing a fixed system magnification would result in spatial resolution degradation within a range of detector angles [6]. The motivation behind the VRX CT design concept is primarily to provide a high spatial resolution, which varies according to the angle between the detector and incident X-ray beam [2]. The influence of focal spot size along with deviation from optimum magnification are the main limiting factors which confine the spatial resolution in the VRX CT scanners [3,6,7].

The spatial resolution improvement can simply be achieved by diminishing the focal spot size but this approach has its own physical limitations [2]. An alternative approach for spatial resolution enhancement in the VRX CT consists of optimizing the magnification at each detector angle [6]. For this purpose, first the optimum magnification at each detector angle should be calculated and then the object should be repositioned accordingly. Changing the position of the object will directly alter the FOV of the system. Therefore, evaluation of the effect of magnification optimization on spatial resolution should be performed along with its impact on the system's FOV [6]. Moreover, the scatter-to-primary ratio of the scanner will vary after magnification optimization owing to changes in object position and FOV of the system. Scattered radiation in VRX CT scanners is of a special importance since the FOV and X-ray tube voltage vary according to object size. Hence, the magnitude and spatial distribution of scatter-to-primary ratio would be different at each detector angle. Furthermore, magnification optimization tends to change the position of the object with respect to the detector and X-ray source which in turn influence the scatter-to-primary ratio.

In current VRX CT scanner configurations, the object position is assumed to be fixed for the entire range of detector angles, which leads to deviation from optimum magnification when the detectors rotate, thus degrading the spatial resolution [6]. In this work, we investigate the influence of magnification optimization on a one-dimensional VRX CT scanner. The spatial resolution, FOV and scatter-to-primary ratio were evaluated for both fixed and optimized magnifications using Monte Carlo simulations [8]. In our previous study [6], we evaluated the trade-off between spatial resolution and transaxial FOV of the scanner as a function of system magnification. Moreover, the limiting effect of the finite size of the X-ray focal spot was also studied in a separate work [5]. In this study, we expand previous contributions by simultaneously evaluating the magnification trade-off between FOV, spatial resolution and scattered radiation using Monte Carlo simulations. Furthermore, the detective quantum efficiency (DQE) of the scanner was computed in order to provide a useful insight into the scanner's performance at different magnifications.

2. Materials and methods

2.1. The VRX CT scanner

Figure 1 depicts a schematic diagram of the VRX CT scanner, which includes a dual-arm VRX detector. In this configuration, the two detector arms can rotate around a common pivotal point (vertex). The dual-arm VRX detector provides left-right symmetry, which is preferable for use in CT scanners. In addition to left-right symmetry, the dual-arm VRX detector provides lower magnification non-uniformity and small variations in the spatial resolution from one end of detector to the other. The dual-arm VRX detector is also suitable for compact system design.

The X-ray source is placed at source-vertex distance from the center of the dual-arm VRX detector. The vertex is a common pivotal point between the two detector arms. The center of the object plane (FOV) is placed at source-object distance from the X-ray source. The diameter of the circle shown in Fig. 1 determines the FOV of the system. The angle between each detector arm and the central axis is called the opening half angle (α). In a VRX CT scanner, the opening half angle changes from almost 90°, where we have the lowest spatial resolution and largest possible FOV, to about 1°, where the spatial resolution reaches its highest value while the FOV is at its smallest range.

2.2. Optimization of magnification

There is a fundamental trade-off between the improvement in detector spatial resolution due to image magnification and

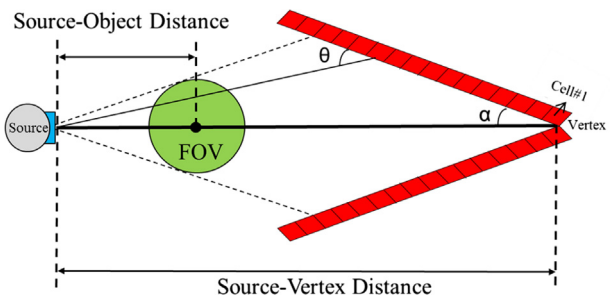

Figure 1. Schematic diagram of a VRX CT scanner; α is the opening half angle and θ the incident angle.

decrease in object detail due to increased source magnification. If the detector cells are defined as a rectangle of width W, the cut-off spatial frequency of the system due only to detector element size is obtained from the following equation.

$$U_d = \frac{M}{W} \quad (1)$$

where M is the system magnification and U_d is the spatial resolution of the scanner due to the effect of detector elements size while other factors such as focal spot, inter-cell cross-talk, and reconstruction algorithm are disregarded. Similarly, the cut-off spatial frequency of the system due to the effect of X-ray focal spot size is obtained from the following equation.

$$U_s = \frac{M}{A(M-1)} \quad (2)$$

where A is the X-ray focal spot size and U_s describes the ideal spatial resolution of the scanner. The system magnification (M) is the common factor in equations (1) and (2) and as such, the optimum magnification for maximum spatial resolution occurs when $U_d = U_s$.

$$M_o = \frac{W}{A} + 1 \quad (3)$$

Both focal spot size and detector spatial resolution influence the overall spatial resolution of the system and the optimal magnification should enable reaching the best achievable spatial resolution. To achieve the highest possible spatial resolution at each opening half angle, it is necessary to reposition the object to satisfy the conditions of optimum magnification and as mentioned earlier, repositioning the object alters the FOV and primary-to-scatter ratio.

2.3. Monte Carlo simulations

A realistic geometrical model of the VRX detector was developed on the GATE (GEANT Application for Tomographic Emission) Monte Carlo platform based on an actual VRX CT scanner designed and built by Melnyk and DiBianca [3]. GATE is a dedicated Monte Carlo package suitable for simulation of medical imaging systems. The first and foremost step in modeling an imaging system in GATE consists in defining its geometry. Owing to the non-conventional geometry of the detectors, a nonstandard model had to be defined. This was achieved using *scanner* generic system in GATE which generates only ASCII and Root outputs. Another important step in the definition of a GATE model is "digitization". In this process, the electronic response of a detector in a scanner is simulated, which involves the conversion of charged particles into an electric signal. Each detector cell was read separately without modeling of time and energy blurring and noise. Since the detectors operate in current mode, no threshold was applied for each individual hit. The total number of detected photons at each detector cell accounted for the cell signal. For the purpose of simplicity and computational load, optical transport was not considered in our simulation.

According to the characteristics of this VRX CT scanner, a fan beam X-ray tube with focal spot size of 0.6 mm was used. The X-ray tube voltage is a function of the FOV in order to produce a decent contrast at minimum patient dose. Based on experimental measurements reported in Ref. [3], the optimum X-ray tube voltage for proper contrast varies nonlinearly from 125 kVp to 40 kVp as the FOV of the VRX CT decreases from 36 cm to 1 cm. This trend of the X-ray tube voltage was used to calculate the spatial resolution and scatter-to-primary ratio where at each opening half angle the FOV of the system is calculated and then the corresponding X-ray energy is obtained from the X-ray tube plot given in Ref. [3]. In the above reference, the optimum X-ray tube voltage was obtained experimentally considering tissue and bone phantoms. The optimum tube voltage obtained from the bone phantom varied from 40 kVp to 70 kVp as the FOV changes from 1 cm to 36 cm. In our simulation, we used the optimum tube voltage obtained from the tissue phantom with the values mentioned earlier. The number of simulated photons was sufficiently high in order to minimize the statistical uncertainties. The *Spektr* tool was used for generation of beam spectra. *Spektr* is a computational tool for X-ray analysis based on the method of interpolating polynominals referred to as *TASMIP* [9]. *Spektr* provides discrete X-ray spectra with a step of 1 keV and maximum energy of 150 keV.

The VRX CT scanner includes two detector arms, each consisting of 12 modules of 24 cells per module (288 cells). The detector cells are composed of cadmium tungstate ($CdWO_4$) having a width of *CelWidth*. The cells are separated by lead (Pb) sheet of width *CelSepWidth.* A reflective paint of width *RefPntWidth* coats the surface between cells and separators. The material of the reflective paint is aluminum oxide (Al_2O_3). The modules are separated by lead sheets of width *ModSepWidth*. The module thickness and height are *ModThick* and *ModHeight*, respectively. Table 1 summarizes the parameters of the detector modules and the VRX CT scanner.

Only one of the detector arms with discrete cells was simulated owing to the left-right symmetry of both arms. The opposite arm was constructed from a uniform material in such a way that the detector had the same X-ray attenuation properties of the original one. This Monte Carlo model was validated in previous studies [7,10].

2.3.1. Calculation of the spatial resolution

The modulation transfer function (MTF) is a standard metric used to characterize the spatial resolution of an imaging system [11]. Evaluation of the system MTF usually involves measurement of the point-spread function (PSF), line-spread function (LSF) or edge-spread function (ESF) [12]. The PSF is defined as the radiation intensity distribution in the image of a point object. Similarly, the LSF and the ESF represent the radiation intensity distribution in the image of a perfectly attenuating line and edge of unit intensity [11,13]. Once the ESF of the system is measured, the corresponding MTF can be computed as [14]:

$$MTF(f) = c\left|F\left(\frac{d}{dx}ESF(x)\right)\right| \quad (4)$$

where F represents the Fourier transform operator, c a normalization constant, x and f are the spatial and frequency coordinates, respectively.

Table 1
Characteristics of the VRX detector module and VRX CT scanner.

VRX detector module parameter	Value
Cell width *CelWidth*	0.79
Module height *ModHeight*	20.14
Module thickness *ModThick*	3.00
Cell separator width *CelSepWidth*	0.10
Module separator width *ModSepWidth*	0.18
Reflective paint width *RefPntWidth*	0.05
VRX CT scanner parameter	
Source-vertex distance	150 cm
Source-object distance	106 cm
Number of cells per arm	288
Number of active cells per arm	256
FOV	1–36 cm
Focal spot size	0.6 cm

In this work, the ESF was used for measurement of the spatial resolution. To fulfill this aim, an edge with infinite attenuation was employed for calculation of the ESF. Technically GATE does not allow using an element with infinite attenuation; however, it is practically possible to define a new element with sufficiently high density to emulate the ideal shield. In our simulation, we defined an element used to build the edge for measuring the ESF having a density 1000 times the density of Tungsten. The edge was placed in front of the middle detector active cell (cell#128) and the radiation intensity distribution of the edge recorded by the detector. In VRX detectors, the variation in magnification of detector cells results in different spatial resolution along the detector length. Cell#1 has the highest magnification while cell#256 (last active cell) has the lowest magnification in the VRX detector. As the opening half angle becomes smaller, the magnification difference between cell#1 and cell#256 increases [3,5]. For instance, at an opening half angle of about 90°, this difference is almost zero while at 23° cell#1 operates at a magnification of 1.41, cell#256 at 1.19 and the middle cell#128 at a magnification of 1.30. The corresponding values at an opening half angle of 6° for cell#1, cell#256 and cell#128 are 1.41, 1.17 and 1.29, respectively. These magnification non-uniformities cause spatial resolution non-uniformity across the detector. The spatial resolution of the VRX detector was measured for cell#128 (middle active cell) since it has a sort of middle magnification along the detector length at each opening half angle. The spatial resolution along the detector varies slowly due to the very small differences in magnification for each cell. Thus, the measured spatial resolution for middle cell#128 is representative of the system spatial resolution. The ESF of the system was measured for 20 opening half angles (α) from 1° to 90° with equal steps.

For each opening half angle, the ESF was calculated twice. First, the object was placed at source-object distance of 106 cm representing the actual configuration of the system and then, the object was placed at optimum magnification. After measurement of the ESF at each opening half angle, the corresponding MTF of each ESF was computed using Eq. (4). Afterwards, the spatial resolution of the system at each opening half angle was extracted from the obtained MTFs. An MTF corresponding to 10% of maximum MTF was used to determine the spatial resolution of the system at each opening half angle.

The spatial resolution of the VRX scanner at a fixed magnification and at optimum magnification was estimated as a function of the opening half angle, thus enabling to assess improvement of the spatial resolution resulting from optimization of magnification.

2.3.2. Calculation of scatter-to-primary ratio

The scatter-to-primary ratio is used as a benchmark for assessment of scattered radiation in computed tomography and is defined as the ratio of scattered radiation occurring in the object to primary X-ray photons recorded by the detector cells [15]. The assessment of the magnitude and spatial distribution of scattered radiation is an important issue in the VRX CT scanner since the FOV (object size) and X-ray tube voltage change at each opening half angle. Furthermore, the detector cells face different distances to the object owing to the angulation of the detector arms [3,5]. This particular feature further diversifies the magnitude and spatial distribution of scattered radiation at each opening half angle. A cylindrical water phantom was used to calculate the scatter-to-primary ratio of the VRX CT scanner as a function of the opening half angle. The phantom had a height of 40 cm and a diameter equal to the FOV of the scanner at the corresponding opening half angle. The same X-ray spectrum used for simulation of spatial resolution was utilized for measurement of scatter. The energy of X-rays at each detector angle is a function of the system's FOV. The scatter-to-primary ratio was calculated for 20 opening half angles with equal steps from 1° to 90°. The scatter-to-primary ratio was calculated twice for each opening half angle. First, the object was placed at a source-object distance of 106 cm (actual configuration of the scanner). Second, the object was placed at optimum magnification. Thereafter, the average of scatter-to-primary ratio for both source-object distances was computed as a function of the opening half angle.

2.3.3. Detective quantum efficiency

At small opening half angles, a considerable amount of the incident photons will more likely be absorbed in the lead cell separator rather than in the scintillator. As such, the detective quantum efficiency (DQE) is thought to be an appropriate characteristic criterion to account for this phenomenon. To this end, the DQE was calculated at each detector angle for both the fixed and optimum magnifications. The following formula was used for calculation of DQE.

$$DQE = \frac{SNR_{out}^2}{SNR_{in}^2} \quad \text{or} \quad DQE(u) = \frac{d^2 \times MTF(u)^2}{q^2 \times NPS(u)}$$

where for a given input flux, d is the average output signal produced, MTF is the measured spatial resolution, q is the number of incident X-ray quanta and NPS indicates the noise power spectrum yielded by the imager at the spatial frequency u.

The output signal to noise ratio (SNR_{out}) is determined by the number of detected photons (d) at each cell which contributes to the output signal multiplied by the measured $MTF(u)$ calculated for the cell under study. The number of detected photons at each detector cell can be simply read from GATE output files and normalized to the defined input flux of X-rays. Conversely, the input signal to noise ratio (SNR_{in}) is simple to calculate given that the number of incident photons on the surface of each detector cell is known. Therefore, the DQE of each detector can be computed separately using the above defined equation.

3. Results

The apparent cells size (W in Eq. (3)) in the VRX CT scanner vary by a factor $1/\sin\theta$ owing to the rotation of detector arms (θ is the angle of incidence of the X-ray beam on the detector) [4]. It can therefore be inferred from Eq. (3) that the optimum magnification changes dramatically when the incident angle changes from 90° to almost 1° [6]. The apparent cells width varies from almost 0.79 mm–0.015 mm as the incident angle changes from 90° to 1°. The variation in apparent cells width leads to different optimum magnification for each opening half angle. The optimum magnification for middle active cell (cell#128) of the VRX detector changes from 2.45 (at opening half angle of 90°) to almost 1.1 (at opening half angle of 1°). The optimum magnification varied non-linearly as a function of the FOV (or opening angle) with values of 1.23, 1.66, 1.93, 2.14 and 2.30 for opening half angles of 10°, 30°, 45°, 60° and 80°, respectively. Optimization of magnification for cell#128 (middle active cell) can greatly reduce the magnification non-uniformity along the detector length [6].

Figure 2 depicts the spatial resolution of the VRX CT versus the opening half angle for a fixed source-object distance of 106 cm and after magnification optimization. The spatial resolution of the VRX scanner was calculated for cell#128 while other detector cells have almost the same spatial resolution at large opening half angles. A relatively large variation was observed at small opening half angles because of the non-uniformity of magnification across the VRX detectors. For instance, at an opening half angle of 23° (at fixed

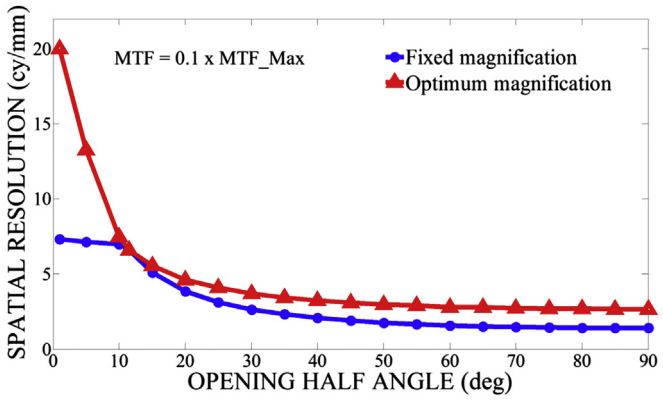

Figure 2. Spatial resolution of the VRX CT scanner at fixed system magnification (source-object distance of 106 cm) and optimized magnification for the middle active cell of the detector (cell#128).

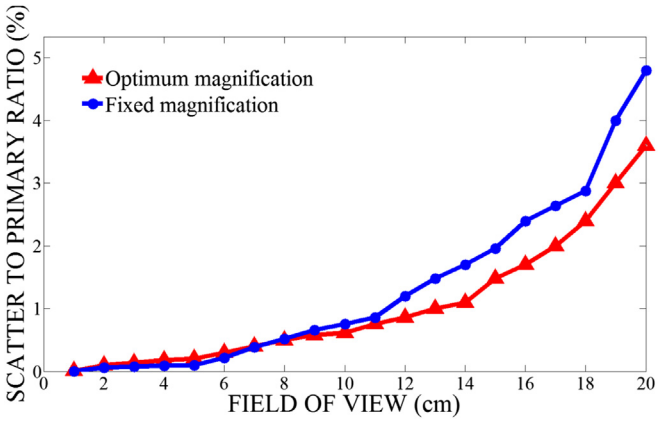

Figure 3. Comparison of scatter-to-primary ratio of the VRX CT scanner for fixed system magnification and optimized magnification at the same FOV (object size) and X-ray energy spectrum.

magnification), the spatial resolution for cell#1, cell#128 and cell#256 were 3.5, 3.2 and 2.9 cy/mm, respectively. These values turned out to be 5.7, 7.5 and 10.7 cy/mm, respectively, at an opening half angle of 6°.

As mentioned earlier, the optimum magnification for cell#128 changes from 2.45 to almost 1.1. Such variation in system magnification entails changing the source-object distance from 62 cm (at opening half angle of 90°) to 130 cm (at opening half angle of 1°). Thus, changing the source-object distance greatly affects the scanner's FOV particularly at large opening half angles where the FOV dropped from 36 cm to 19 cm at 90° and from 26 cm to 16 cm at 40°. On the other hand, the FOV tended to increase at small opening half angles (below 12°) after optimization of magnification.

Likewise, both the source-object distance and scanner's FOV had significant impact on the scatter-to-primary ratio. Initially, the comparison of scatter-to-primary ratio before and after magnification optimization was performed based upon the common opening half angle. . This comparison was not straightforward in the sense that the comparison is not performed using the same object size and simulated X-ray energy spectrum. The significant reduction of scatter after optimization of magnification originated from the decrease in object size and effective X-ray energy. To put into perspective the sole impact of magnification changes on the amount of scattered radiation, the comparison was made using the same object size and X-ray spectrum as illustrated in Fig. 3. It is worth to highlight that the relative contribution of photoelectric and Compton interaction cross-sections to the attenuation of X-rays in water as a function of photon energy plays a role in this context. Indeed, by increasing the X-ray energy (range: 40 keV–140 keV), the number of scattered radiation tends to decrease nonlinearly. Therefore, at a given FOV and same object-to-detector distance, the scatter-to-primary ratio increases as the X-ray energy increases. For instance, at a FOV of 20 cm, the scatter-to-primary ratio is 11.9%, 6.7%, 4.8% and 3.2% at X-ray energies of 80, 100, 125 and 140 keV, respectively.

Figure 4 depicts the relative DQE as a function of the detector angle. At each detector angle, the DQE corresponding to 1/10th of the maximum DQE is plotted in Fig. 4 similar to MTF plots. Figure 5 shows the percentage of change in the FOV, scatter-to-primary ratio and spatial resolution of the VCT scanner after optimization of magnification in comparison to fixed system magnification. Optimization of magnification had opposing effects on the FOV, scatter-to-primary ratio and spatial resolution and involves a trade-off between these factors in the VRX CT scanner.

4. Discussion

The rationale behind the design of the VRX CT scanner is to provide a variable spatial resolution as a function of the opening half angle along with achieving comparatively high spatial resolution at small opening half angles. The spatial resolution at opening half angles between 90° and 12° is a sinusoidal function of the opening half angle (Fig. 2). However, at opening half angles below 12°, the spatial resolution was limited by the focal spot size. The influence of focal spot size restricted the spatial resolution of the system to almost 7.5 cy/mm. Although at angles below 12°, the apparent cells width in the object plane were considerably small enabling the spatial resolution reach up to 40 cy/mm [3], the focal spot size played the dominant role and limited the achievable spatial resolution. The slight variation in spatial resolution at angles below 12° stems from the relatively small changes in system magnification because of detector rotation. At opening half angles between 90° and 12°, the detector resolution was the limiting factor of spatial resolution and the focal spot size had minor effect. Thus, the spatial resolution is improved owing to improvement in detector resolution achieved by its angulation. The optimization of magnification had two appreciable effects on the spatial resolution: first, the spatial resolution improves significantly especially at small opening half angles from 7.5 cy/mm to almost 20 cy/mm. Second, the spatial resolution becomes a sinusoidal function of the opening half angle for the whole range of α.

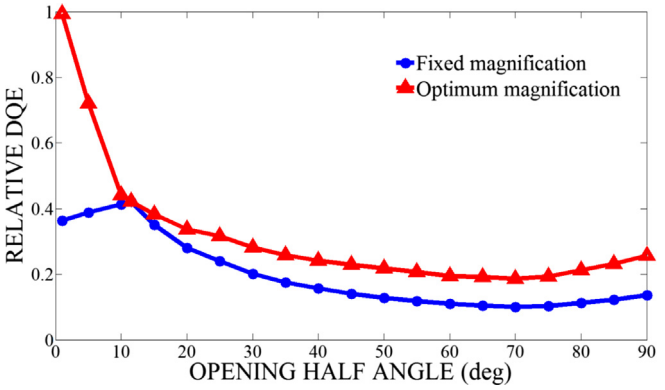

Figure 4. Relative detective quantum efficiency (DQE) at each detector opening half angle for fixed and optimized magnification. All values are normalized to the maximum DQE at a FOV of 1 cm at optimum magnification.

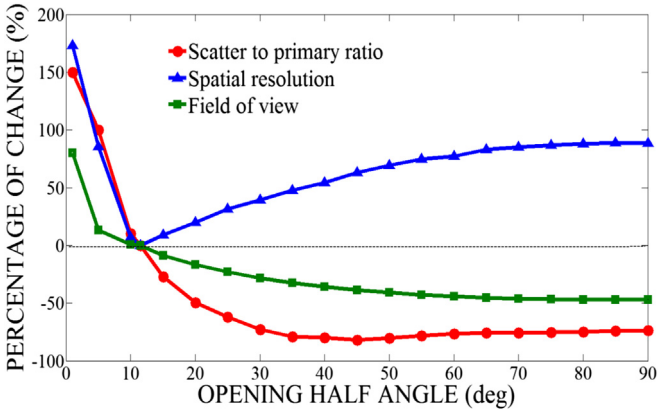

Figure 5. The percentage of changes in spatial resolution, field-of-view and scatter-to-primary ratio of the VRX CT scanner after optimization of magnification at each opening half angle.

The plot of the relative system DQE demonstrate almost a similar behavior to the MTF. At small angles, the DQE show significant improvement owing to the improvement in spatial resolution after optimization of magnification. At fixed magnification, the DQE exhibit a downward behaviour. The motive of this trend is twofold: first at small detector angles there is no improvement in spatial resolution (the MTF is almost constant), and second, at small detector angles the incident photons flux encounter the detector surface at very oblique angles and as such, they face a smaller effective length in the scintillation crystals and are more likely to be absorbed in lead cell separators. A similar effect is observed at large detector angles where despite the improved spatial resolution compared to a detector angle of 90°, the DQE decrease owing to the higher possibility for the incident photons to pass through the scintillation crystal and interact in the lead separators.

For the VRX CT with a source-object distance of 106 cm, the magnification was optimum for an angle of ~12°. At opening half angles ranging between 90° and 12°, the optimum magnification was higher than the magnification adopted in the experimental configuration. A higher magnification entails reducing the source-object distance which in turn changes the FOV of the scanner. Therefore, optimization of magnification at opening half angles of 90°–12° reduces the FOV of the scanner by up to 50%. On the contrary, the optimum magnification for opening half angles of below 12° was lower than the system magnification. Thus, increasing the source-object distance led to enlargement of the FOV.

After optimization of magnification, the scatter-to-primary ratio decreased significantly at large opening half angles (from 14% to 4%). The decrease in scatter-to-primary ratio after optimization of magnification is due to the reduction in the size of the FOV (object size) and at the same time a lower X-ray effective energy. The decrease in scatter-to-primary ratio was beyond expectation after optimization of magnification. This can be partially justified by reduction of the FOV; however, changing the object-detector distance had also major impact on scatter-to-primary ratio. After optimization of magnification, the source-object distance changed from 106 cm to 130 cm at opening half angle of 90°. When the object is placed at larger distance from the detector, scattered radiation has a lower probability of reaching the detector especially for single array detectors. Therefore, the scatter-to-primary ratio tends to decrease at larger object-detector distances. This effect can be seen in Fig. 3 where the comparison is made using the same object size and X-ray spectrum with the only variant being the object to detector distance. The scattered radiation tends to increase at small FOVs after optimization of magnification because of closer object distance to the detector, however, the contribution of scattered radiation for these FOVs is still less than 1%.

The optimization of magnification in the VRX CT at opening half angles of 90°–12°, not only decreases the FOV, but also increases the object-detector distance. Both factors cause significant reduction in scatter-to-primary ratio at these angles. The optimization of magnification at opening half angles below 12° increases the FOV as well as the source-object distance. Both factors contribute to increasing the scatter-to-primary ratio.

5. Conclusion

The focal spot size limits the spatial resolution of the VRX CT scanner to 7.5 cy/mm. In addition, at opening half angles below 12°, the spatial resolution remains set independent of detector angulation. After optimization of magnification at each opening half angle, the spatial resolution increases up to 20 cy/mm. Moreover, optimization of magnification minimizes the deteriorating effect of focal spot size on spatial resolution, which becomes a function of the opening half angle for the whole range of α. Optimization of magnification at each opening half angle of the VRX CT scanner introduces a trade-off between spatial resolution, FOV and scatter-to-primary ratio. After optimization of magnification at opening half angles ranging between 90° and 12°, the spatial resolution improvement is achieved at the expense of considerable reduction in the scanners' FOV (up to 50%). Beside the improvement in spatial resolution, the scatter-to-primary ratio decreases from over 4.8%–3.8% at the same FOV (object size) and X-ray energy spectrum. On the other hand, optimization of magnification for opening half angles below 12° increases both the FOV and spatial resolution at the expense of a higher scatter-to-primary ratio. At small opening half angles, the scatter-to-primary ratio was under 1%, even after optimization of magnification. Hence, optimization of magnification is essential for opening half angles below 12° because it increases the FOV and spatial resolution while the scatter-to-primary ratio is still acceptably small. For opening half angles of 90°–12°, the magnification should be set according to the desired spatial resolution, FOV and importance of scattered radiation.

Acknowledgments

This work was supported by the Swiss National Science Foundation under grant SNSF 31003A-149957.

References

[1] Wang G, Zhao S, Yu H, Miller C, Abbas P, Gantz B, et al. Design, analysis and simulation for development of the first clinical micro-CT scanner. Acad Radiol 2005;12:511–25.
[2] DiBianca FA, Zou P, Jordan LM, Laughter JS, Zeman HD, Sebes J. A variable resolution X-ray detector for computed tomography: II. Imaging theory and performance. Med Phys 2000;27:1875–80.
[3] Melnyk R, DiBianca FA. Modeling and measurement of the detector presampling MTF of a variable resolution X-ray CT scanner. Med Phys 2007;34:1062–75.
[4] Jordan LM, DiBianca FA, Melnyk R, Choudhary A, Shukla H, Laughter J, et al. Determination of calibration parameters of a VRX CT system using an 'Amoeba' algorithm. J X-Ray Sci Technol 2004;12:281–93.
[5] Arabi H, Kamali Asl AR, Aghamiri SM. The effect of focal spot size on the spatial resolution of variable resolution X-ray CT scanner. Iran J Radiat Res 2010;8(1):37–43.
[6] Kamali Asl AR, Arabi H, Tamhidi S. Optimization of magnification in a VRX CT scanner. IFMBE Proc 2009;25(2):266–9.
[7] Arabi H, Kamali Asl AR. A novel method based on Monte Carlo for simulation of variable resolution X-ray CT scanner: measurement of system presampling MTF. World Acad Sci Eng Technol 2010;44:969–73.
[8] Zaidi H, Ay MR. Current status and new horizons in Monte Carlo simulation of X-ray CT scanners. Med Biol Eng Comput 2007;45:809–17.
[9] Boone JM, Seibert JA. An accurate method for computergenerating tungsten anode X-ray spectra from 30 to 140 kV. Med Phys 1997;24:1661–70.

[10] Arabi H, Asl AR, Ay MR, Zaidi H. Novel detector design for reducing intercell x-ray cross-talk in the variable resolution X-ray CT scanner: a Monte Carlo study. Med Phys 2011;38:1389–96.
[11] Rossmann K. Point spread-function, line spread-function, and modulation transfer function. Tools for the study of imaging systems. Radiology 1969;93:257–72.
[12] Khodadad D, Ahmadian A, Ay MR, Esfahani AF, Banaem HY, Zaidi H. B-spline based free form deformation thoracic non-rigid registration of CT and PET images. 1-3 October 2011. In: International Conference on Graphic and Image Processing (ICGIP 2011). 1st ed. Cairo, Egypt: SPIE; 2011. p. 82851.
[13] Greer PB, van Doorn T. Evaluation of an algorithm for the assessment of the MTF using an edge method. Med Phys 2000;27:2048–59.
[14] Samei E, Ranger NT, Dobbins JTI, Chen Y. Intercomparison of methods for image quality characterization. I. Modulation transfer function. Med Phys 2006;33:1454–65.
[15] Endo M, Tsunoo T, Nakamori N, Yoshida K. Effect of scattered radiation on image noise in cone beam CT. Med Phys 2001;28:469–74.